Modal Analysis of Discontinuities Between Elliptical Waveguides

Mauro Mongiardo and Cristiano Tomassoni

***Abstract*—Elliptical waveguides are currently finding applications in several components as corrugated horns, cavities for dual-mode filters and feeds for reflector antennas since they provide improved flexibility, better manufacturability, and higher Q with respect to either circular or rectangular waveguides. Efficient computer-aided design of components involving elliptical waveguides requires rapid evaluation of the scattering parameters at the discontinuities. To this end, we derive analytical formulas for full-wave study of a general junction between two elliptical waveguides and the relative specialization to the case of a junction between a circular and concentrical elliptical waveguide of larger cross section. With respect to current approaches, which are generally based on the numerical evaluation of the coupling integrals, the proposed analytical formulas allow to achieve a significant reduction of computer time. Results have been tested against published data and have also been compared with data obtained by numerical evaluation of the coupling integrals; in all cases, an almost perfect agreement has been observed.**

***Index Terms*—Elliptical waveguide, mode matching, waveguide discontinuities.**

I. INTRODUCTION

Elliptical waveguides have recently found application in a variety of microwave components: their use has been proposed for dual-mode filters [1], as low sensitivity irises, as wide-band transmission lines, etc. Waveguide discontinuities involving elliptical structures have received limited attention thus far: the case of a junction between two confocal elliptical waveguides has been considered in [2], the general step discontinuity between two elliptical waveguides has been studied in [3], while the problem of the junction between rectangular and elliptical waveguides has been considered in [4] and [5]; junctions between concentrical elliptical and circular waveguides have been investigated in [5] for the cross section of the circular waveguide enclosing that of the elliptical waveguide. A different technique that approximate the boundary conditions by a set of sinusoidal functions has been proposed in [6]. Elliptical waveguides radiating into free space have been considered in [7] and [8], where a transition between a rectangular waveguide and an elliptical one radiating into a half-space was studied. Recently, in [2] and [5], the modal coupling coefficients have been obtained by analytical formulas. The approach proposed in [6] results in being convenient for modest values of the eccentricity since it approximate the field in the elliptical waveguide by means of sinusoidal functions, which are the natural expansions for circular waveguides. Moreover, when a high accuracy is required, such as in the case of design of narrow-band filters, a considerable number of modes should be considered; unfortunately, in this approach, no warranty is given on the accuracy of the computed higher order modes.

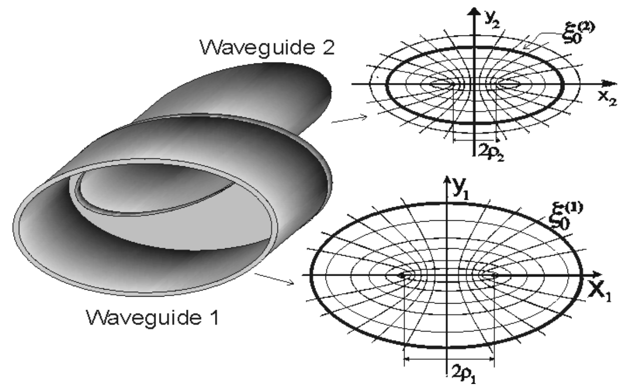

Fig. 1. General junction between two elliptical waveguides. Note that, for the modal expansion, we use a different elliptical coordinate system for each waveguide. The waveguide and related elliptical coordinate system have the same semifocal length.

In this paper, we present the detailed derivation of some analytical formulas for modal coupling integrals evaluation for the general junction between two elliptical waveguides (see Fig. 1). We provide an explicit analytical solution of the coupling integrals appeared in [3] which, as discussed later, allow a significant reduction of computing time. These formulas can be specialized to the particular case of the junction between a circular and an elliptical waveguide of larger cross section; moreover, in this case, it is also possible to obtain a single-term expression for the coupling coefficients that does not require computation of Mathieu functions.

In Section II, we present the theoretical evaluation of the coupling coefficients for the case of two elliptical waveguides. In Section III, we specialize the results to the case of the junction between a circular and an elliptical waveguide. Finally, in Section IV, we compare the results of the proposed approach with published and reference data.

II. THEORY

A. Modal Analysis in Elliptical Waveguides

Modal analysis of the step discontinuity between two elliptical waveguides requires knowledge of the relative modal spectra, i.e., the solution of the Helmholtz equation in elliptical coordinates. In particular, it can be found [10], [11] that the longitudinal component of the electromagnetic field $\psi(\xi, \eta)$

Manuscript received November 4, 1999.

The authors are with the Dipartimento di Ingegneria Elettronica e dell'Informazione, Università di Perugia, I-06100 Perugia, Italy (e-mail: mongiard@unipg.it).

Publisher Item Identifier S 0018-9480(00)02776-9.

(i.e., E_z or H_z) in an elliptical waveguide of semifocal length ρ can be written as a product of Mathieu functions (ce, se) and modified Mathieu functions (Ce, Se).

In order to introduce notation, we denote (see Fig. 1) by ρ_i the semifocal length of the ith waveguide (where $i = 1, 2$), and $h_i = \rho_i K_c^{(i)}$ (where $K_c^{(i)}$ is the cutoff wavenumber of the ith waveguide). The parameter $K_c^{(i)}$ is chosen to satisfy boundary conditions for TE or TM modes. Accordingly, the potentials are written in terms of even and odd solutions of the Helmholtz equation, shown in (1) and (2), at the bottom of this page [9], [10]. In the above formulas, the symbol $'$ is referred to TM modes, while the symbol $''$ is referred to TE modes, superscript E and O are referred to even and odd functions, respectively, the index i is referred to the ith waveguide, and $\xi^{(i)}$ and $\eta^{(i)}$ are the radial and angular coordinates, respectively, of an elliptical coordinate system of semifocal length $\rho = \rho_i$. Moreover, N_i is the normalization constant and $K_{n_i,\ell_i}^{(i)}$ is the cutoff wavenumber of the mode in the ith waveguide. Finally, $\mathrm{TM}_{n,m}^E$ and $\mathrm{TE}_{n,m}^E$ are the even modes, while $\mathrm{TM}_{n,m}^O$ and $\mathrm{TE}_{n,m}^O$ are the odd modes.

For future use, it is expedient to express the Mathieu functions appearing in (1) and (2) by considering the following trigonometric expansions:

$$ce_{2m+np}(h,\eta) = \sum_{r=0}^{\infty} A_{h,2r+np}^{(2m+np)} \cos\Big[(2r+np)\eta\Big]$$
$$se_{2m+np}(h,\eta) = \sum_{r=0}^{\infty} B_{h,2r+np}^{(2m+np)} \sin\Big[(2r+np)\eta\Big]. \quad (3)$$

In the above equations $m = 1, 2, 3, \cdots,\ np = 0, 1$ and the series expansion coefficients A and B are calculated as in ([11, pp. 557–567]) and normalized as in ([11, p. 1568]), i.e.,

$$\sum_{r=0}^{\infty} A_{h,2r+np}^{(2m+np)} = 1 \qquad \sum_{r=0}^{\infty} (2r+np) B_{h,2r+np}^{(2m+np)} = 1. \quad (4)$$

By using the same expansion coefficients A and B, we can also express the modified Mathieu functions in terms of Bessel functions as

$$Ce_{2m+np}(h,\xi) = \sqrt{\frac{\pi}{2}} \sum_{r=0}^{\infty} (-1)^{r-m} \times A_{h,2r+np}^{(2m+np)} J_{2r+np}(h\cosh\xi)$$
$$Se_{2m+np}(h,\xi) = \sqrt{\frac{\pi}{2}} \tanh(\xi) \sum_{r=0}^{\infty} (-1)^{r-m} \times (2r+np) B_{h,2r+np}^{(2m+np)} J_{2r+np}(h\cosh\xi). \quad (5)$$

B. Change of Coordinates

For the evaluation of the coupling integrals of the general step between two elliptical waveguides, it is expedient to use only the elliptical coordinate system of the waveguide with smaller cross section; hence, we write the potential of waveguide 1 in the elliptical coordinate system used for waveguide 2.

To this end, we apply the following procedure.

1) We express the modal function of the larger waveguide (written in the elliptical coordinate system 1) in plane-wave expansions in the rectangular coordinate system of guide 1 (see Section II-B.1).
2) The plane waves are now rewritten in terms of the rectangular coordinate system of guide 2 (see Section II-B.2).
3) We now expand each of the above plane waves in terms of the elliptical eigenfunction pertaining to the (elliptical) coordinate system 2 (see Section II-B.3).

The above procedure is illustrated in detail in the following sections and the modes of guide 1 are expanded in the eigenfunctions of the elliptical coordinate system 2 in Section II-B.4, with the relative expansion coefficients given in Section II-B.5.

1) Plane-Wave Expansions of Modes in Guide 1: Using the relations [10] and [11, p. 1422, eq. (11.2.95)]

$$\left\{ \begin{array}{l} Ce_{2m_1+np_1}\left(\rho_1 k_c, \xi^{(1)}\right) ce_{2m_1+np_1}\left(\rho_1 k_c, \eta^{(1)}\right) \\ Se_{2m_1+np_1}\left(\rho_1 k_c, \xi^{(1)}\right) se_{2m_1+np_1}\left(\rho_1 k_c, \eta^{(1)}\right) \end{array} \right\} = \frac{1}{j^{2m_1+np_1}\sqrt{8\pi}} \int_0^{2\pi} e^{jk_c[x_1\cos u + y_1 \sin u]} \times \left\{ \begin{array}{l} ce_{2m_1+np_1}(\rho_1 k_c, u) \\ se_{2m_1+np_1}(\rho_1 k_c, u) \end{array} \right\} du. \quad (6)$$

Here, the point (x_1, y_1) in rectangular coordinates translates in a point $(\xi^{(1)}, \eta^{(1)})$ in elliptical coordinates of semifocal length ρ_1.

2) Plane Waves in Rectangular Coordinate System 2: Equation (6) can be written in terms of the rectangular coordinate system of guide 2, changing the coordinate system of the plane wave (see Fig. 2), i.e.,

$$e^{jk_c[x_1\cos u + y_1\sin u]} = e^{jk_c r_o \cos(u-\psi_o)} \times e^{jk_c\left[x_2\cos(u-\psi_o) + y_2 \sin(u-\psi_o)\right]}. \quad (7)$$

$$\psi_{n_i,\ell_i}'^{(i)^{E/O}}\left(\xi^{(i)},\eta^{(i)}\right) = \left\{ \begin{array}{l} N_i Ce_{n_i}\left(\rho_i K_{n_i,\ell_i}'^{(i)E}, \xi^{(i)}\right) ce_{n_i}\left(\rho_i K_{n_i,\ell_i}'^{(i)E}, \eta^{(i)}\right) \Rightarrow \mathrm{TM}_{n_i,\ell_i}^E \\ N_i Se_{n_i}\left(\rho_i K_{n_i,\ell_i}'^{(i)O}, \xi^{(i)}\right) se_{n_i}\left(\rho_i K_{n_i,\ell_i}'^{(i)O}, \eta^{(i)}\right) \Rightarrow \mathrm{TM}_{n_i,\ell_i}^O \end{array} \right. \quad (1)$$

$$\psi_{n_i,\ell_i}''^{(i)^{E/O}}\left(\xi^{(i)},\eta^{(i)}\right) = \left\{ \begin{array}{l} N_i Ce_{n_i}\left(\rho_i K_{n_i,\ell_i}''^{(i)E}, \xi^{(i)}\right) ce_{n_i}\left(\rho_i K_{n_i,\ell_i}''^{(i)E}, \eta^{(i)}\right) \Rightarrow \mathrm{TE}_{n_i,\ell_i}^E \\ N_i Se_{n_i}\left(\rho_i K_{n_i,\ell_i}''^{(i)O}, \xi^{(i)}\right) se_{n_i}\left(\rho_i K_{n_i,\ell_i}''^{(i)O}, \eta^{(i)}\right) \Rightarrow \mathrm{TE}_{n_i,\ell_i}^O \end{array} \right. \quad (2)$$

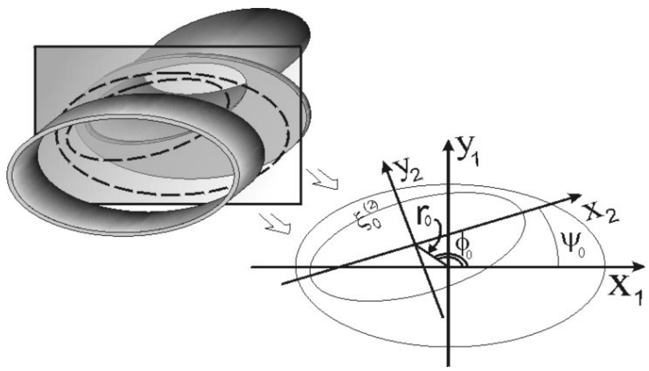

Fig. 2. Coordinate systems on the discontinuity plane. Due to the generality of the discontinuity, the coordinate system 2 (related to waveguide 2) is rotated (ψ_o) and translated (r_o, ϕ_o) with respect to the coordinate system 1 (related to waveguide 1).

3) Plane Waves in Terms of Elliptical Eigenfunctions: According to [10] and ([11, p. 1422, eq. (11.2.94)], the plane waves in (7) can be written as

$$\begin{aligned} &e^{jk_c\left[x_2\cos(u-\psi_o)+y_2\sin(u-\psi_o)\right]} \\ &\quad= \sqrt{8\pi}\sum_{m=0}^{\infty}\sum_{np=0}^{1} j^{2m+np} \\ &\qquad\times\left\{\left[\frac{ce_{2m+np}(\rho_2k_c,u-\psi_o)}{M^E_{2m+np}(\rho_2k_c)}\right]\right. \\ &\qquad\quad\times Ce_{2m+np}\left(\rho_2k_c,\xi^{(2)}\right)ce_{2m+np}\left(\rho_2k_c,\eta^{(2)}\right) \\ &\qquad\quad+\left[\frac{se_{2m+np}(\rho_2k_c,u-\psi_o)}{M^O_{2m+np}(\rho_2k_c)}\right] \\ &\qquad\quad\left.\times Se_{2m+np}\left(\rho_2k_c,\xi^{(2)}\right)se_{2m+np}\left(\rho_2k_c,\eta^{(2)}\right)\right\}. \end{aligned} \tag{8}$$

The point (x_2, y_2) in rectangular coordinates translates in a point $(\xi^{(2)}, \eta^{(2)})$ in elliptical coordinates of semifocal length ρ_2, while [accordingly with (3)]

$$\begin{aligned} M^E_{2m+np}(h) &= \int_0^{2\pi}\left|ce_{2m+np}(h,\eta)\right|^2 d\eta \\ &= \pi\sum_{r=0}^{\infty}\left|A^{(2m+np)}_{h,2r+np}\right|^2\epsilon^2_{2r+np} \end{aligned} \tag{9}$$

$$\begin{aligned} M^O_{2m+np}(h) &= \int_0^{2\pi}\left|se_{2m+np}(h,\eta)\right|^2 d\eta \\ &= \pi\sum_{r=0}^{\infty}\left|B^{(2m+np)}_{h,2r+np}\right|^2 \end{aligned} \tag{10}$$

where

$$\epsilon_i = \begin{cases}\sqrt{2}, & \text{if } i=0\\ 1, & \text{otherwise}\end{cases}$$

and the $M^E_{2m+np}(h)$, $M^O_{2m+np}(h)$ are the normalization constants of the Mathieu functions.

4) Modes in Guide 1 Expanded in Eigenfunctions of Elliptical Coordinate System 2: Inserting (8) in (7) and (7) in (6)

$$\begin{aligned} &\begin{Bmatrix} Ce_{2m_1+np_1}\left(\rho_1k_c,\xi^{(1)}\right)ce_{2m_1+np_1}\left(\rho_1k_c,\eta^{(1)}\right)\\ Se_{2m_1+np_1}\left(\rho_1k_c,\xi^{(1)}\right)se_{2m_1+np_1}\left(\rho_1k_c,\eta^{(1)}\right)\end{Bmatrix} \\ &\quad= \pi\sum_{m=0}^{\infty}\sum_{np=0}^{1}(-1)^{m-m_1+np(1-np_1)} \\ &\qquad\times\left[\begin{Bmatrix}\Lambda^{ee}_{m,np}\\ \Lambda^{oe}_{m,np}\end{Bmatrix}Ce_{2m+np}\left(\rho_2k_c,\xi^{(2)}\right)\right. \\ &\qquad\quad\times ce_{2m+np}(\rho_2k_c,\eta^{(2)}) \\ &\qquad\quad+\begin{Bmatrix}\Lambda^{eo}_{m,np}\\ \Lambda^{oo}_{m,np}\end{Bmatrix}Se_{2m+np}(\rho_2k_c,\xi^{(2)}) \\ &\qquad\quad\left.\times se_{2m+np}\left(\rho_2k_c,\eta^{(2)}\right)\right] \end{aligned} \tag{11}$$

where the Λ coefficients are defined as

$$\begin{aligned} \begin{Bmatrix}\Lambda^{ee}_{m,np}\\ \Lambda^{oe}_{m,np}\end{Bmatrix} &= \frac{j^{-np_o}}{\pi M^E_{2m+np}(\rho_2k_c)}\int_0^{2\pi}e^{jk_cr_o\cos(u-\psi_o)} \\ &\quad\times\begin{Bmatrix}ce_{2m_1+np_1}(\rho_1k_c,u)\\ se_{2m_1+np_1}(\rho_1k_c,u)\end{Bmatrix} \\ &\quad\times ce_{2m+np}(\rho_2k_c,u-\psi_o)\,du \end{aligned} \tag{12}$$

$$\begin{aligned} \begin{Bmatrix}\Lambda^{eo}_{m,np}\\ \Lambda^{oo}_{m,np}\end{Bmatrix} &= \frac{j^{-np_o}}{\pi M^O_{2m+np}(\rho_2k_c)}\int_0^{2\pi}e^{jk_cr_o\cos(u-\psi_o)} \\ &\quad\times\begin{Bmatrix}ce_{2m_1+np_1}(\rho_1k_c,u)\\ se_{2m_1+np_1}(\rho_1k_c,u)\end{Bmatrix} \\ &\quad\times se_{2m+np}(\rho_2k_c,u-\psi_o)\,du \end{aligned} \tag{13}$$

with

$$np_o = \begin{cases}0, & \text{if } np_1 = np\\ 1, & \text{if } np_1 \neq np.\end{cases}$$

The Λ coefficients can be evaluated in closed form, as will be show in the following section.

5) Λ Coefficients in Closed Form: The integrals appearing in (12) and (13) can be evaluated in closed form. As an example, we solve the case for $\Lambda^{ee}_{m,np}$. As a first step, we write the product $ce_{2m_1+np_1}(\rho_1k_c,u)ce_{2m+np}(\rho_2k_c,u-\psi_o)$ as sin and cos expansion (Fourier expansion). To this end, with the aid of (3), we write

$$\begin{aligned} &ce_{2m_1+np_1}(\rho_1k_c,u)ce_{2m+np}(\rho_2k_c,u-\psi_o) \\ &\quad= \frac{1}{4}\sum_{p=-\infty}^{\infty}\left[\epsilon^2_{|p|}A^{(2m_1+np_1)}_{h,|p|}\right]e^{-jpu} \\ &\qquad\times\sum_{\ell=-\infty}^{\infty}\left[\epsilon^2_{|\ell|}A^{(2m+np)}_{h,|\ell|}e^{j\ell\psi_o}\right]e^{-jpu}. \end{aligned} \tag{14}$$

The above equation can be seen as a product of the discrete Fourier transform (DFT) of the discrete sequences in square brackets; this mean that the entire product can be seen as the DFT of the convolution $C^{ee}[q]$ of the above discrete sequences, i.e.,

$$\begin{aligned} &ce_{2m_1+np_1}(\rho_1k_c,u)ce_{2m+np}(\rho_2k_c,u-\psi_o) \\ &\qquad= \frac{1}{4}\sum_{q=-\infty}^{\infty}C^{ee}[q]e^{-jpu} \end{aligned} \tag{15}$$

where the convolution $C^{ee}[q]$ is defined as

$$C^{ee}[q]=\sum_{\tau=-\infty}^{\infty}\left[\epsilon^2_{|q-\tau|}A^{(2m_1+np_1)}_{h,|q-\tau|}\right]\times\left[\epsilon^2_{|\tau|}A^{(2m+np)}_{\hat{h},|\tau|}e^{j\tau\psi_o}\right]. \tag{16}$$

The above equation can be conveniently separated into real and imaginary part, as illustrated in (21). The following Fourier expansion can be obtained:

$$\begin{aligned}&ce_{2m_1+np_1}(\rho_1 k_c,u)ce_{2m+np}(\rho_2 k_c,u-\psi_o)\\&=\frac{1}{2}\left[\sum_{q=0}^{\infty}\frac{C^{ee}_{\rm Re}[2q+np_o]}{\epsilon^2_{2q+np_o}}\cos[(2q+np_o)u]\right.\\&\left.\quad+\sum_{q=1-np_o}^{\infty}C^{ee}_{\rm Im}[2q+np_o]\sin[(2q+np_o)u]\right].\end{aligned} \tag{17}$$

Finally, inserting (17) into the first of (12) with the aid of [11, p. 1371, eq. (11.2.21)], i.e.,

$$\begin{Bmatrix}\cos(m\Phi_o)\\ \sin(m\Phi_o)\end{Bmatrix}\frac{J_m(k_c r_o)}{2\pi j^m}=\int_0^{2\pi}e^{jk_c r_o\cos(u-\Phi_o)}\begin{Bmatrix}\cos(mu)\\ \sin(mu)\end{Bmatrix}du \tag{18}$$

the first of (19) can be found.

Following the same procedure, all other Λ coefficients can be found as follows:

$$\begin{aligned}\begin{Bmatrix}\Lambda^{ee}_{m,np}\\ \Lambda^{oe}_{m,np}\end{Bmatrix}&=\sum_{q=0}^{\infty}(-1)^q\frac{J_{2q+np_o}(k_c r_o)}{M^E_{2m+np_1}(\rho_2 k_c)}\\&\times\left[\begin{Bmatrix}C^{ee}_{\rm Re}[2q+np_o]\\ C^{oe}_{\rm Re}[2q+np_o]\end{Bmatrix}\right.\\&\times\frac{1}{\epsilon^2_{|2q+np_o|}}\cos\left[(2q+np_o)\phi_o\right]\\&\left.+\begin{Bmatrix}C^{ee}_{\rm Im}[2q+np_o]\\ C^{oe}_{\rm Im}[2q+np_o]\end{Bmatrix}\sin\left[(2q+np_o)\phi_o\right]\right]\end{aligned} \tag{19}$$

$$\begin{aligned}\begin{Bmatrix}\Lambda^{eo}_{m,np}\\ \Lambda^{oo}_{m,np}\end{Bmatrix}&=\sum_{q=0}^{\infty}(-1)^q\frac{J_{2q+np_o}(k_c r_o)}{M^O_{2m+np_1}(\rho_2 k_c)}\\&\times\left[\begin{Bmatrix}C^{eo}_{\rm Re}[2q+np_o]\\ C^{oo}_{\rm Re}[2q+np_o]\end{Bmatrix}\right.\\&\times\frac{1}{\epsilon^2_{|2q+np_o|}}\cos[(2q+np_o)\phi_o]\\&\left.+\begin{Bmatrix}C^{eo}_{\rm Im}[2q+np_o]\\ C^{eo}_{\rm Im}[2q+np_o]\end{Bmatrix}\sin\left[(2q+np_o)\phi_o\right]\right]\end{aligned} \tag{20}$$

while the C coefficients can be evaluated as follows:

$$\begin{aligned}\begin{Bmatrix}C^{ee}_{\rm Re}[q]\\ C^{ee}_{\rm Im}[q]\end{Bmatrix}&=\sum_{\tau=-\infty}^{\infty}\begin{Bmatrix}\cos\left[(2\tau+np)\psi_o\right]\\ \sin\left[(2\tau+np)\psi_o\right]\end{Bmatrix}\\&\times\left[\epsilon^2_{|2\tau+np|}A^{(2m+np)}_{\hat{h},|2\tau+np|}\right]\\&\times\left[\epsilon^2_{|q-2\tau-np|}A^{(2m_1+np_1)}_{h_1,|q-2\tau-np|}\right]\end{aligned} \tag{21}$$

$$\begin{aligned}\begin{Bmatrix}C^{oo}_{\rm Re}[q]\\ C^{oo}_{\rm Im}[q]\end{Bmatrix}&=-\sum_{\tau=-\infty}^{\infty}\begin{Bmatrix}\cos\left[(2\tau+np)\psi_o\right]\\ \sin\left[(2\tau+np)\psi_o\right]\end{Bmatrix}\\&\times\left[\frac{2\tau+np}{|2\tau+np|}B^{(2m+np)}_{\hat{h},|2\tau+np|}\right]\\&\times\left[\frac{q-2\tau-np}{|q-2\tau-np|}B^{(2m_1+np_1)}_{h_1,|q-2\tau-np|}\right]\end{aligned} \tag{22}$$

$$\begin{aligned}\begin{Bmatrix}C^{eo}_{\rm Re}[q]\\ C^{eo}_{\rm Im}[q]\end{Bmatrix}&=\sum_{\tau=-\infty}^{\infty}\begin{Bmatrix}-\sin\left[(2\tau+np)\psi_o\right]\\ \cos\left[(2\tau+np)\psi_o\right]\end{Bmatrix}\\&\times\left[\frac{2\tau+np}{|2\tau+np|}B^{(2m+np)}_{\hat{h},|2\tau+np|}\right]\\&\times\left[\epsilon^2_{|q-2\tau-np|}A^{(2m_1+np_1)}_{h_1,|q-2\tau-np|}\right]\end{aligned} \tag{23}$$

$$\begin{aligned}\begin{Bmatrix}C^{oe}_{\rm Re}[q]\\ C^{oe}_{\rm Im}[q]\end{Bmatrix}&=\sum_{\tau=-\infty}^{\infty}\begin{Bmatrix}-\sin\left[(2\tau+np)\psi_o\right]\\ \cos\left[(2\tau+np)\psi_o\right]\end{Bmatrix}\\&\times\left[\epsilon^2_{|2\tau+np|}A^{(2m+np)}_{\hat{h},|2\tau+np|}\right]\\&\times\left[\frac{q-2\tau-np}{|q-2\tau-np|}B^{(2m_1+np_1)}_{h_1,|q-2\tau-np|}\right].\end{aligned} \tag{24}$$

Note that the formulas of (11), specialized for $k_c=K^{(1)}_{n_1,\ell_1}$, provide the expression of the modal fields in the larger waveguide (waveguide 1) in terms of the coordinate system of the waveguide of smaller cross section (waveguide 2). Equation (11) is the basis for the closed-form evaluation of the modal coupling coefficients considered in the following section.

C. Coupling Integrals

The generic coupling integral is defined as

$$g_{p,q}=\int_{\mathcal{S}_2}\mathbf{e}^{(1)}_p\cdot\mathbf{e}^{(2)}_q\,ds \tag{25}$$

where $\mathcal{S}_2$ is the cross section of the elliptical waveguide 2, p stands for a particular n_1, ℓ_1, $'$ or $''$, E or O combination, while q stands for a particular n_2, ℓ_2, $'$ or $''$, E or O combination. Using (1), (2), and (11), we can solve the coupling integral (25) in elliptical coordinate of semifocal length ρ_2. In this coordinate system, the boundary of $\mathcal{S}_2$ is described by a single coordinate $\xi^{(2)}=\xi^{(2)}_0$ (see Fig. 2) and the following formulas hold.

For TM modes $\begin{array}{l}\mathrm{TM}^{(1)E/O}_{2m_1+np_1,\ell_1} - \mathrm{TM}^{(2)E}_{2m_2+np_2,\ell_2}\\ \mathrm{TM}^{(1)E/O}_{2m_1+np_1,\ell_1} - \mathrm{TM}^{(2)O}_{2m_2+np_2,\ell_2}\end{array}$

$$g_{p,q} = \frac{N_1 N_2 \pi^2 \hat{h}^2}{\hat{h}^2 - h_2^2}\frac{d}{d\xi}\begin{Bmatrix} Ce_{2m_2+np_2}\left(h_2, \xi_0^{(2)}\right)\\ Se_{2m_2+np_2}\left(h_2, \xi_0^{(2)}\right)\end{Bmatrix} \times \sum_{m=0}^{\infty}(-1)^{m-m_1+np_2(1-np_1)} \times \begin{Bmatrix}\Lambda^{ee/oe}_{m,np_2} Ce_{2m+np_2}\left(\hat{h}, \xi_0^{(2)}\right)\\ \Lambda^{eo/oo}_{m,np_2} Se_{2m+np_2}\left(\hat{h}, \xi_0^{(2)}\right)\end{Bmatrix} \times \sum_{r=0}^{\infty}\begin{Bmatrix} A^{(2m+np_2)}_{\hat{h},2r+np_2} A^{(2m_2+np_2)}_{h_2,2r+np_2}\epsilon^2_{2r+np_2}\\ B^{(2m+np_2)}_{\hat{h},2r+np_2} B^{(2m_2+np_2)}_{h_2,2r+np_2}\end{Bmatrix}. \quad (26)$$

For TE modes $\begin{array}{l}\mathrm{TE}^{(1)E/O}_{2m_1+np_1,\ell_1} - \mathrm{TE}^{(2)E}_{2m_2+np_2,\ell_2}\\ \mathrm{TE}^{(1)E/O}_{2m_1+np_1,\ell_1} - \mathrm{TE}^{(2)O}_{2m_2+np_2,\ell_2}\end{array}$

$$g_{p,q} = \frac{N_1 N_2 \pi^2 h_2^2}{h_2^2 - \hat{h}^2}\begin{Bmatrix} Ce_{2m_2+np_2}\left(h_2, \xi_0^{(2)}\right)\\ Se_{2m_2+np_2}\left(h_2, \xi_0^{(2)}\right)\end{Bmatrix} \times \sum_{m=0}^{\infty}(-1)^{m-m_1+np_2(1-np_1)} \times \frac{d}{d\xi}\begin{Bmatrix}\Lambda^{ee/oe}_{m,np_2} Ce_{2m+np_2}\left(\hat{h}, \xi_0^{(2)}\right)\\ \Lambda^{eo/oo}_{m,np_2} Se_{2m+np_2}\left(\hat{h}, \xi_0^{(2)}\right)\end{Bmatrix} \times \sum_{r=0}^{\infty}\begin{Bmatrix} A^{(2m+np_2)}_{\hat{h},2r+np_2} A^{(2m_2+np_2)}_{h_2,2r+np_2}\epsilon^2_{2r+np_2}\\ B^{(2m+np_2)}_{\hat{h},2r+np_2} B^{(2m_2+np_2)}_{h_2,2r+np_2}\end{Bmatrix}. \quad (27)$$

In the case of TM modes in waveguide 1 and TE in waveguide 2

$\begin{array}{l}\mathrm{TM}^{(1)E/O}_{2m_1+np_1,\ell_1} - \mathrm{TE}^{(2)E}_{2m_2+np_2,\ell_2}\\ \mathrm{TM}^{(1)E/O}_{2m_1+np_1,\ell_1} - \mathrm{TE}^{(2)O}_{2m_2+np,\ell_2}\end{array}$

$$g_{p,q} = N_1 N_2 \pi^2 \begin{Bmatrix} -Ce_{2m_2+np_2}\left(h_2, \xi_0^{(2)}\right)\\ Se_{2m_2+np_2}\left(h_2, \xi_0^{(2)}\right)\end{Bmatrix} \times \sum_{m=0}^{\infty}(-1)^{m-m_1+np_2(1-np_1)} \times \begin{Bmatrix}\Lambda^{eo/oo}_{m,np_2} Se_{2m+np_2}\left(\hat{h}, \xi_0^{(2)}\right)\\ \Lambda^{ee/oe}_{m,np_2} Ce_{2m+np_2}\left(\hat{h}, \xi_0^{(2)}\right)\end{Bmatrix} \times \sum_{r=0}^{\infty}(2r+np)\begin{Bmatrix} B^{(2m+np_2)}_{\hat{h},2r+np_2} A^{(2m_2+np_2)}_{h_2,2r+np_2}\\ A^{(2m+np_2)}_{\hat{h},2r+np_2} B^{(2m_2+np_2)}_{h_2,2r+np_2}\end{Bmatrix}. \quad (28)$$

Finally, in all other cases

$$g_{p,q} = 0. \quad (29)$$

Here, $\hat{h} = \rho_2 K^{(1)}_{n_1,\ell_1}$, while $h_2 = \rho_2 K^{(2)}_{n_1,\ell_1}$.

TABLE I

	$TE^{(2)E}$	$TE^{(2)O}$	$TM^{(2)E}$	$TM^{(2)O}$
$TE^{(1)E}$	x	0	0	0
$TE^{(1)O}$	0	x	0	0
$TM^{(1)E}$	0	x	x	0
$TM^{(1)O}$	x	0	0	x

D. Concentrical Elliptical Waveguides

In the particular case of concentrical waveguides ($r_o = 0$), by taking advantage of the fact that

$$J_n(0) = \begin{cases} 1, & \text{if } n = 1\\ 0, & \text{if } n \neq 0\end{cases} \quad (30)$$

we obtain from (19) and (20) the following relations:

$$\Lambda^{ee/oe}_{m,np} = \Lambda^{oe/oo}_{m,np} = 0, \qquad \text{if } np \neq np_1. \quad (31)$$

The above equation states that, for $np_1 \neq np_2$, the modes in waveguide 1 with first index $2m_1 + np_1$ are not coupled with the mode in waveguide 2 having $2m_2 + np_2$ as a first index.

Moreover, if the two waveguides are concetrical ($r_o = 0$) and collinear (i.e., with the axes in the same direction, $\psi_o = 0$), the following useful expressions for the relevant coefficients hold:

$$\begin{aligned} &\Lambda^{eo}_{m,np} = \Lambda^{oe}_{m,np} = 0\\ &\Lambda^{ee}_{m,np} = \frac{\sum_{r=0}^{\infty} A^{(2m+np)}_{\hat{h},2r+np} A^{(2m_1+np_1)}_{h_1,2r+np}\epsilon^2_{2r+np}}{M^E_{2m+np}(\hat{h})}\\ &\qquad \Rightarrow \text{if } np = np_1\\ &\Lambda^{oo}_{m,np} = \frac{\sum_{r=0}^{\infty} B^{(2m+np)}_{\hat{h},2r+np} B^{(2m_1+np_1)}_{h_1,2r+np}}{M^O_{2m+np}(\hat{h})}\\ &\qquad \Rightarrow \text{if } np = np_1\\ &\Lambda^{ee}_{m,np} = \Lambda^{oo}_{m,np} = 0 \quad \Rightarrow \text{if } np \neq np_1. \end{aligned} \quad (32)$$

From the above equations, it is verified that, for collinear waveguides, several coefficients vanish, as illustrated in Table I, where the "x"' denotes a nonzero coefficient (for $np_1 = np_2$).

In the case of confocal waveguides, it is noted that the above formulas specialize to the results presented in [2].

III. Junction Between the Elliptical and Circular Waveguides

By considering the circular waveguide as a limiting case of an elliptical waveguide, several useful relationships can be obtained, as reported in the Appendix. By using the latter expressions, we can specialize (26)–(29) in order to evaluate in a closed form the coupling integrals arising when considering the junction between concentrical elliptical and circular waveguides.

With the aid of (9) (10), (32), and (41)–(46), we can write (26)–(29) for $\rho_2 \to 0$ as follows.

For TM modes

$$\mathrm{TM}^{(e)E}_{2m_1+np,\ell_1} - \mathrm{TM}^{(c)E}_{2m_2+np,\ell_2}, \quad \mathrm{TM}^{(e)O}_{2m_1+np,\ell_1} - \mathrm{TM}^{(c)O}_{2m_2+np,\ell_2}$$

$$g_{p,q} = \frac{(-1)^\nu \epsilon_i \pi N {k_c^{(e)}}^2}{{k_c^{(e)}}^2 - {k_c^{(c)}}^2} \times \begin{Bmatrix} A^{(2m_1+np)}_{h_1,i} \\ B^{(2m_1+np)}_{h_1,i} \end{Bmatrix} \frac{J_i'\left(k_c^{(c)} r_0\right)}{\left|J_i'\left(k_c^{(c)} r_0\right)\right|} J_i\left(k_c^{(e)} r_0\right). \quad (33)$$

For TE modes

$$\mathrm{TE}^{(e)E}_{2m_1+np,\ell_1} - \mathrm{TE}^{(c)E}_{2m_2+np,\ell_2}, \quad \mathrm{TE}^{(e)O}_{2m_1+np,\ell_1} - \mathrm{TE}^{(c)O}_{2m_2+np,\ell_2}$$

$$g_{p,q} = \frac{(-1)^\nu \epsilon_i N {k_c^{(c)}}^2}{{k_c^{(c)}}^2 - {k_c^{(e)}}^2} \begin{Bmatrix} A^{(2m_1+np)}_{h_1,i} \\ B^{(2m_1+np)}_{h_1,i} \end{Bmatrix} \times \frac{\pi k_c^{(e)} r_0}{\sqrt{\left(k_c^{(c)} r_0\right)^2 - i^2}} \frac{J_i\left(k_c^{(c)} r_0\right)}{\left|J_i\left(k_c^{(c)} r_0\right)\right|} J_i'\left(k_c^{(e)} r_0\right). \quad (34)$$

In the case of TM modes in elliptical waveguide and TE in circular waveguide

$$\mathrm{TM}^{(e)E}_{2m_1+np,\ell_1} - \mathrm{TE}^{(c)O}_{2m_2+np,\ell_2}, \quad \mathrm{TM}^{(e)O}_{2m_1+np,\ell_1} - \mathrm{TE}^{(c)E}_{2m_2+np,\ell_2}$$

$$g_{p,q} = \begin{Bmatrix} A^{2m_1+np}_{h_1,i} \\ -B^{2m_1+np}_{h_1,i} \end{Bmatrix} \times \frac{(-1)^\nu N i \pi}{\sqrt{\left(k_c^{(c)} r_0\right)^2 - i^2}} \frac{J_i\left(k_c^{(c)} r_0\right)}{\left|J_i\left(k_c^{(c)} r_0\right)\right|} J_i\left(k_c^{(e)} r_0\right). \quad (35)$$

Finally, in all other cases

$$g_{p,q} = 0 \quad (36)$$

where $i = 2m_2 + np$, $\nu = m_2 - m_1$, and $k_c^{(e)}$ represents the cutoff wavenumber in elliptical waveguide, $k_c^{(c)}$ is the cutoff wavenumber in circular waveguide, N is the normalization constant of the mode in elliptical waveguide, and $J_n'(x)$ is the first derivative of the Bessel function of order n $J_n(x)$. For the circular waveguide, the *odd* modes, are the degenerate of the *even* modes.

The above formulas, with respect to the case of two concentrical elliptical waveguides, are very useful and simple to understand: the sum is vanished and the modified Mathieu function have been replaced by Bessel functions.

With considerations analogous to those used for the evaluation of (33)–(36), we can find the coupling integrals in the case of the step between a circular and an elliptical waveguide of smaller cross section, i.e., the results published in [5].

A. An Alternative Approach

There is also another way to directly find the relations (33)–(36), i.e., by inserting (3) into (6) and by bringing the sum out of the sign of integral, with the aid of (18), we can solve (6) analytically as follows:

$$Ce_{2m_1+np_1}\left(\rho_1 k_c, \xi^{(1)}\right) ce_{2m_1+np_1}\left(\rho_1 k_c, \eta^{(1)}\right) = \sqrt{\frac{\pi}{2}} \sum_{r=0}^{\infty} (-1)^{r+m_1} A^{(2m_1+np_1)}_{\rho_1 k_c, 2r+np} \times \cos\left\{(2r+np)\phi\right\} J_{2r+np}(k_c r) \quad (37)$$

$$Se_{2m_1+np_1}\left(\rho_1 k_c, \xi^{(1)}\right) se_{2m_1+np_1}\left(\rho_1 k_c, \eta^{(1)}\right) = \sqrt{\frac{\pi}{2}} \sum_{r=0}^{\infty} (-1)^{r+m_1} B^{(2m_1+np_1)}_{\rho_1 k_c, 2r+np} \times \sin\left\{(2r+np)\phi\right\} J_{2r+np}(k_c r) \quad (38)$$

where the point $(\xi^{(1)}, \eta^{(1)})$ in elliptical coordinates of semi-focal length ρ_1 translates in a point (r, ϕ) in circular coordinates. Now, by using (37) and (38) in order to represent $\mathbf{e}_p^{(1)}$ and by using the potential of circular waveguide in order to represent $\mathbf{e}_q^{(2)}$ in (25), we finally obtain the relations (33)–(36).

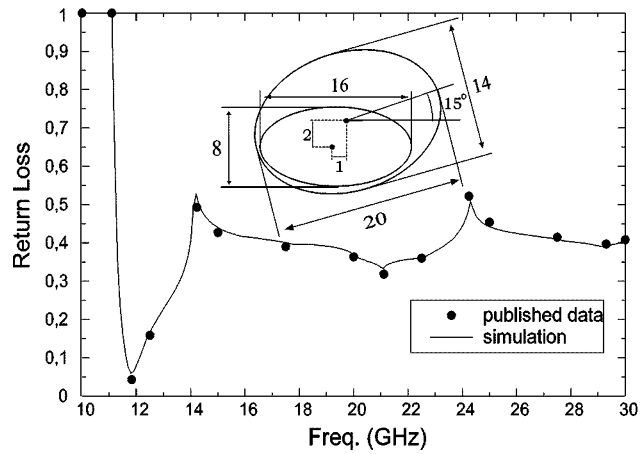

Fig. 3. Return loss of the junction between two elliptical waveguides. The geometrical dimensions are reported (in millimeters) in the inset. Published data refer to [3] where a numerical evaluation of the coupling integrals was used.

IV. Results

In order to check the usefulness of the presented formulas, we have considered several waveguide junctions and compared the results with published data. In particular, Fig. 3 reports the reflection coefficient of a junction between two elliptical waveguides and the data published in [3], showing an excellent agreement.

Fig. 4 illustrates the reflection coefficient relative to the discontinuity between an elliptical waveguide and a concentrical circular waveguide of smaller cross section. Results have been obtained by using (33)–(36) relative to the step between concentrical elliptical and circular waveguides. By considering the circular waveguide as a limiting case of the elliptical waveguide, i.e., for a very small eccentricity (in our case, $e = 0.01$), it is also possible to employ, for comparison purposes, (26)–(29) specialized with the relations of (32) to the concentrical elliptical waveguide case. Moreover, results have also been verified by performing the numerical integration of the coupling integrals. For the latter, as far as numerical accuracy is concerned,

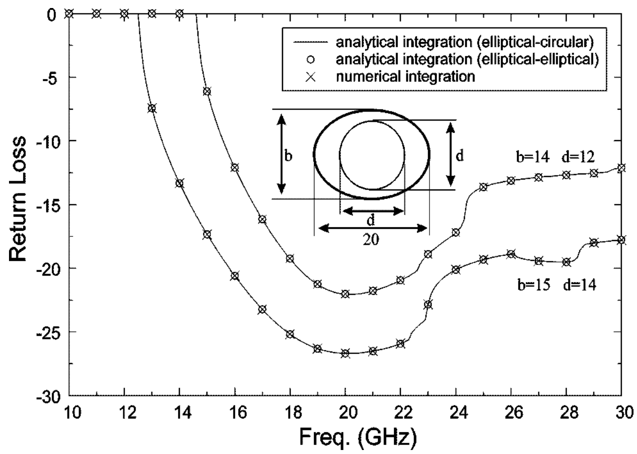

Fig. 4. As in Fig. 3, but in this case, the waveguide of smaller cross section is a circular one. Comparison has been made by analytical formulas and numerical integration.

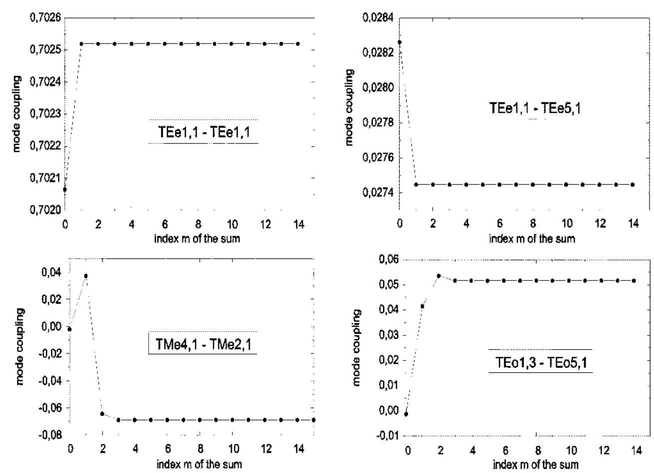

Fig. 5. Convergence behavior of the sums of (26)–(28) for different mode coupling. The modal indexes are reported in the inset; the first one refers to the mode in the waveguide of larger cross section. A significant rapidity of convergence is apparent. The same type of convergence is also achieved for concentrical waveguides.

a perfect agreement (up to four decimal digits for the coupling integrals) is noted for all three of the approaches considered.

In order to ascertain the numerical efficiency of the proposed approach, we have developed a code that makes use of the coupling integrals expressions reported in [3]. The numerical performances of this code have been compared with a code that implements the analytical expressions introduced in this study. For a single frequency point, the code based on the analytical integration is about 40 times faster than the code based on the numerical integration; as an example, the case reported in Fig. 3, where 80 frequency points have been computed, has required 105 s on a PC Pentium II (200 MHz).

Since a summation sign is present in (26)–(28) for the coupling coefficients relative to the junction between two elliptical waveguides, it is of interest to ascertain the convergence behavior of these sums. In Fig. 5, we have plotted such converge behavior for the discontinuity considered in Fig. 3; the modal functions considered are reported in the inset (the first mode refers to the larger waveguide). From Fig. 5, a noticeable rapidity of convergence is apparent. In the worst cases, we need

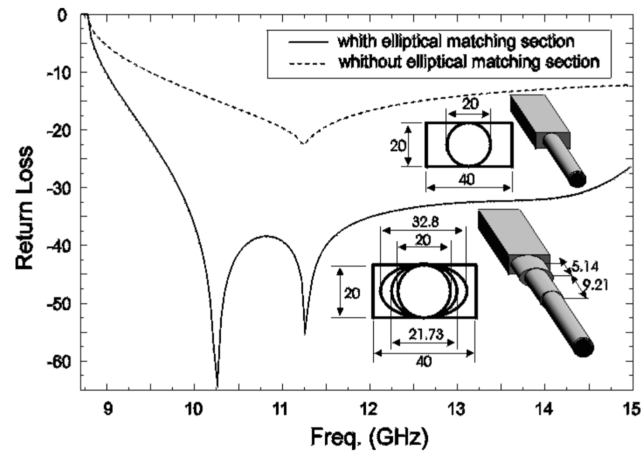

Fig. 6. Optimized return loss for the junction between a circular and rectangular waveguide. Matching is achieved by using two intermediate sections of elliptical waveguide with dimensions determined by optimization.

about three terms in the sums, while in several instances, just the first term of the sum suffices.

The high numerical efficiency of the formulas introduced in this study makes them very suitable for practical applications in optimization routines where, at each iteration, the geometrical dimensions and, therefore, the coupling integrals, are changed. As an example, we have considered the junction between a circular and rectangular waveguide, shown in the inset of Fig. 6. In order to achieve a matched condition in the frequency band of interest, it is convenient to place a couple of sections of elliptical waveguides between the circular and rectangular waveguides. By using a suitable optimization routine, it is possible to achieve a fairly good match, as illustrated in Fig. 6, at the cost of a modest numerical effort.

V. Conclusion

We have presented an analytical solution for the efficient computer-aided design (CAD) of junctions between elliptical waveguides. The coupling coefficients are evaluated by a rapidly convergent sum. Computed results have been compared with published data and with other data obtained by numerical integration; in all cases, an almost perfect agreement has been observed. However, the code based on the analytical expression of the coupling coefficients has proven to be significantly faster than the code based on the numerical evaluation of the coupling integrals.

Appendix
Conversion from Elliptical to Circular Coordinates

In an elliptical coordinate system (ξ, η) of semifocal length ρ, the semimajor axis a and semiminor axis b of an ellipse are given by

$$a = \rho \cosh \xi \quad b = \rho \sinh \xi. \tag{39}$$

By fixing the semimajor axis of the ellipse at the value $\bar{a}$ with ρ approaching zero, we note that the elliptical coordinate ξ, which characterizes the ellipse of semimajor axis $\bar{a}$, goes to infinity and the ellipse becomes a circle of radius $r = \bar{a}$, where [see (39)]

$$r = \lim_{\rho \to 0} \rho \cosh \xi = \lim_{\rho \to 0} \rho \sinh \xi. \tag{40}$$

For $h \rightarrow 0$, it is easy to demonstrate that (see [10] and [11])

$$\lim_{\rho\rightarrow 0} ce_{2m+np}(h,\eta) = \cos\Big[(2r+np)\eta\Big] \quad (41)$$

$$\lim_{\rho\rightarrow 0} se_{2m+np}(h,\eta) = \frac{1}{2m+np}\sin\Big[(2r+np)\eta\Big]$$

and from (4) and (41)

$$A_{2r+np}^{(2m+np)} \overset{\rho\rightarrow 0}{\longrightarrow} \begin{cases} 1, & \text{if } r=m \\ 0, & \text{if } r\neq m \end{cases}$$

$$B_{2r+np}^{(2m+np)} \overset{\rho\rightarrow 0}{\longrightarrow} \begin{cases} \dfrac{1}{2r+np}, & \text{if } r=m \\ 0, & \text{if } r\neq m. \end{cases} \quad (42)$$

Inserting (40) and (42) in (5), and remembering that $h=\rho k_c$ and $\tanh(\xi)=1$ when $\xi\rightarrow\infty$, we can write

$$\lim_{\rho\rightarrow 0}\begin{Bmatrix} Ce_{2m+np}(h,\xi) \\ Se_{2m+np}(h,\xi)\end{Bmatrix} = \sqrt{\frac{\pi}{2}}J_{2m+np}(k_c r) \quad (43)$$

and

$$\lim_{\rho\rightarrow 0}\frac{d}{d\xi}\begin{Bmatrix} Ce_{2m+np}(h,\xi) \\ Se_{2m+np}(h,\xi)\end{Bmatrix} = \lim_{\rho\rightarrow 0}\sqrt{\frac{\pi}{2}}h\sinh(\xi)J'_{2m+np}(h\cosh\xi) = \sqrt{\frac{\pi}{2}}k_c r J'_{2m+np}(k_c r). \quad (44)$$

In the elliptical coordinate system, when $\rho\rightarrow 0$, the angular elliptical coordinate $\eta\rightarrow\phi$, where ϕ is the angular coordinate of a circular coordinate system (r,ϕ). At this point, two considerations can be made. The first is that the potential as $\rho\rightarrow 0$ is the product of a Bessel function for a $\sin$ or $\cos$ function (that is the potential of the circular waveguide). The second consideration is that the odd modes in an elliptical waveguide become the degenerate modes in a circular waveguide (angular potential depending on $\sin$ functions).

Applying the relation (41) and (43) at the potential of waveguide 2 when $\rho_2\rightarrow 0$, the normalization constant N_2 can be evaluated analytically as follows.

For TM modes

$$\lim_{\rho_2\rightarrow 0} N_2 = \begin{cases} \dfrac{\frac{2}{\pi}\frac{1}{\epsilon_i}}{k_c^{(c)}r_o\left|J'_i\left(k_c^{(c)}r_o\right)\right|} \Rightarrow \mathrm{TM}_{2m_2+np,\ell_2}^{(c)E} \\ \dfrac{\frac{2}{\pi}\frac{i}{\epsilon_i}}{k_c^{(c)}r_o\left|J'_i\left(k_c^{(c)}r_o\right)\right|} \Rightarrow \mathrm{TM}_{2m_2+np,\ell_2}^{(c)O}. \end{cases} \quad (45)$$

For TE modes

$$\lim_{\rho_2\rightarrow 0} N_2 = \begin{cases} \dfrac{\frac{2}{\pi}\frac{1}{\epsilon_i}}{\sqrt{\left(k_c^{(c)}r_o\right)^2-(i)^2}\left|J_i\left(k_c^{(c)}r_o\right)\right|} \Rightarrow \mathrm{TE}_{2m_2+np,\ell_2}^{(c)E} \\ \dfrac{\frac{2}{\pi}\frac{i}{\epsilon_i}}{\sqrt{\left(k_c^{(c)}r_o\right)^2-(i)^2}\left|J_i\left(k_c^{(c)}r_o\right)\right|} \Rightarrow \mathrm{TE}_{2m_2+np,\ell_2}^{(c)O}. \end{cases} \quad (46)$$

where $i=2m_2+np$, $k_c^{(c)}$ is the cutoff wavenumber of the mode in waveguide 2 and

$$r_0 = \lim_{\rho_2\rightarrow 0}\rho_2\cosh\xi_0^{(2)}$$

is the radius of the waveguide 2.

ACKNOWLEDGMENT

The authors would like to thank the reviewers for their useful comments.

REFERENCES

[1] L. Accatino, G. Bertin, and M. Mongiardo, "Elliptical cavity resonators for dual-mode narrowband filters," *IEEE Trans. Microwave Theory Tech.*, vol. 45, pp. 2393–2401, Dec. 1997.

[2] P. Matras, R. Bunger, and F. Arndt, "Mode-matching analysis of the step discontinuity in elliptical waveguides," *IEEE Microwave Guided Wave Lett.*, vol. 6, pp. 143–145, Mar. 1996.

[3] ——, "Modal scattering matrix of the general step discontinuity in elliptical waveguides," *IEEE Trans. Microwave Theory Tech.*, vol. 45, pp. 453–458, Mar. 1997.

[4] M. Dionigi, M. Mongiardo, C. Tomassoni, and M. Vernata, "Modal analysis of discontinuities between elliptical and rectangular waveguides," in *IEEE AP-S Int. Symp.*, Montreal, P.Q., Canada, July 1997, pp. 1426–1429.

[5] K.-L. Chan and S. R. Judah, "Two-port scattering at an elliptic-waveguide junction," *IEEE Trans. Microwave Theory Tech.*, vol. 45, pp. 1255–1262, Aug. 1997.

[6] B. Gimeno and M. Guglielmi, "Full-wave network representation for rectangular, circular, and elliptical to elliptical waveguide junctions," *IEEE Trans. Microwave Theory Tech.*, vol. 45, pp. 376–384, Mar. 1997.

[7] T. S. Bird, "Behaviour of multiple elliptical waveguides opening into a ground plane," *Proc. Inst. Elect. Eng.*, vol. 137, pp. 121–126, Apr. 1990.

[8] L. B. Felsen, M. Mongiardo, P. Russer, G. Conti, and C. Tomassoni, "Waveguide component analysis by a generalised network approach," in *European Microwave Conf.*, Sept. 1997, pp. 949–954.

[9] L. J. Chu, "Electromagnetic waves in elliptic hollow pipes of metal," *J. Appl. Phys.*, vol. 9, pp. 583–591, Sept. 1938.

[10] N. W. McLachlan, *Theory and Application of Mathieu Functions* Dover, New York, 1974.

[11] P. M. Morse and H. Feshbach, *Methods of Theoretical Physics*. New York: McGraw-Hill, 1953.

Mauro Mongiardo received the Laurea degree (*summa cum laude*) from the University of Rome, Rome, Italy, in 1983, and the Ph.D. degree from the University of Bath, Bath, U.K., in 1991.

He is currently an Associate Professor at the University of Perugia, Perugia, Italy. He has been Visiting Scientist at the University of Victoria, Victoria, B.C., Canada, the University of Bath, Oregon State University, Corvallis, and the Technical University of Munich, Munich, Germany. His main contributions are in the area of modeling of waveguide discontinuities, both in the cases of closed waveguides and open waveguides, such as microstrip lines or coplanar waveguides. His research interests include numerical methods with contributions in the areas of mode-matching techniques, integral equations, variational techniques, finite difference time domain (FDTD), transmission-line matrix (TLM), and finite-element method (FEM). He is also involved with frequency- and time-domain analysis of monolithic microwave integrated circuits (MMIC's) and is currently interested in the modeling and computer-aided procedures for the design of microwave and millimeter-wave components.

Cristiano Tomassoni was born in Italy, in 1969. He received the Laurea degree from the University of Perugia, Perugia, Italy, in 1996, and is currently working toward the Ph.D. degree at the University of Perugia.

He is currently a Visiting Scientist with the Technical University of Munich, Munich, Germany. His research interests include the modeling of waveguide discontinuities and the modeling of open-ended waveguides radiating in a half-space. He is currently interested in hybrid methods in the modeling and design of microwave components.